Chapter 11

Mechanical and Metalurgical Properties of Friction Welded Aluminium Joints

Mumin Sahin and Cenk Misirli

Additional information is available at the end of the chapter

http://dx.doi.org/10.5772/51130

1. Introduction

Aluminium alloys are alloys in which aluminium (Al) is the predominant metal. The typical alloying elements are copper, magnesium, manganese, silicon and zinc. There are two principal classifications, namely casting alloys and wrought alloys, both of which are further subdivided into the categories heat-treatable and non-heat-treatable. About 85% of aluminium is used for wrought products, for example rolled plate, foils and extrusions. Cast aluminium alloys yield cost effective products due to the low melting point, although they generally have lower tensile strengths than wrought alloys. The most important cast aluminium alloy system is Al-Si, where the high levels of silicon (4.0% to 13%) contribute to give good casting characteristics. Aluminium alloys are widely used in engineering structures and components where light weight or corrosion resistance is required [1].

Light non-ferrous metals such as aluminium and magnesium alloys have drawn attention with regard to application due to their energy-saving character. Above all, aluminium alloys are used more due to their superior workability and less cost. However, they are not entirely replaced by stainless steel, stainless steel having superior strength and weldability in certain structures. Therefore, it is necessary to join stainless steel and aluminium materials. Then, copper - aluminium joints are inevitable for certain applications due to unique performances such as higher electric conductivity, heat conductivity, corrosion resistance and mechanical properties. Aluminium and copper are replacing steels in electricity supply systems due to higher electric conductivity.

Friction welding is used extensively in various industries. Heat in friction welding is generated by conversion of mechanical energy into thermal energy at the interface of work pieces during rotation under pressure. Various ferrous and non-ferrous alloys having circular or non-circular cross sections and that have different thermal and mechanical properties can

easily be joined by friction welding method. Friction welding is classified as a solid-state welding process where metallic bonding is produced at temperatures lower than the melting point of the base metals. Friction time, friction pressure, forging time, forging pressure and rotation speed are the most important parameters in the friction welding method [2].

In practice, friction welding is classified in two ways; continuous drive friction welding and inertia friction welding [3, 4]. In the continuous drive friction method (Figure 1), one of the components is held stationary while the other is rotated at a constant speed (s). The two components are brought together under axial pressure (P_f) for a certain friction time (t_f). Then, the clutch is separated from the drive, and the rotary component is brought to stop within the braking time while the axial pressure on the stationary part is increased to a higher upset pressure (P_u) for a predetermined upset time (t_u). Parameters of the method are shown in Figure 2.

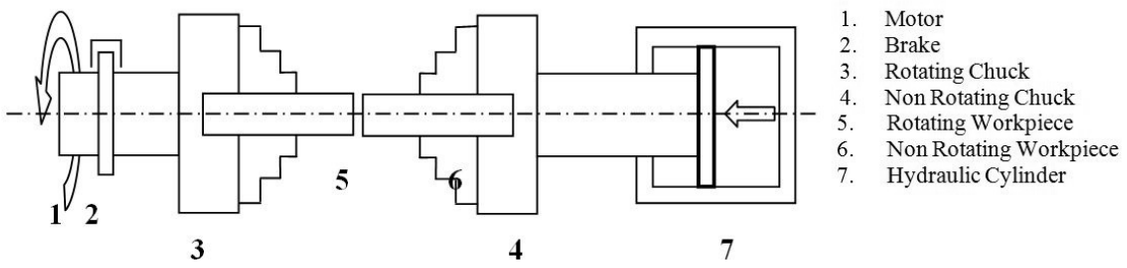

Figure 1. Layout of Continuous Drive Friction Welding

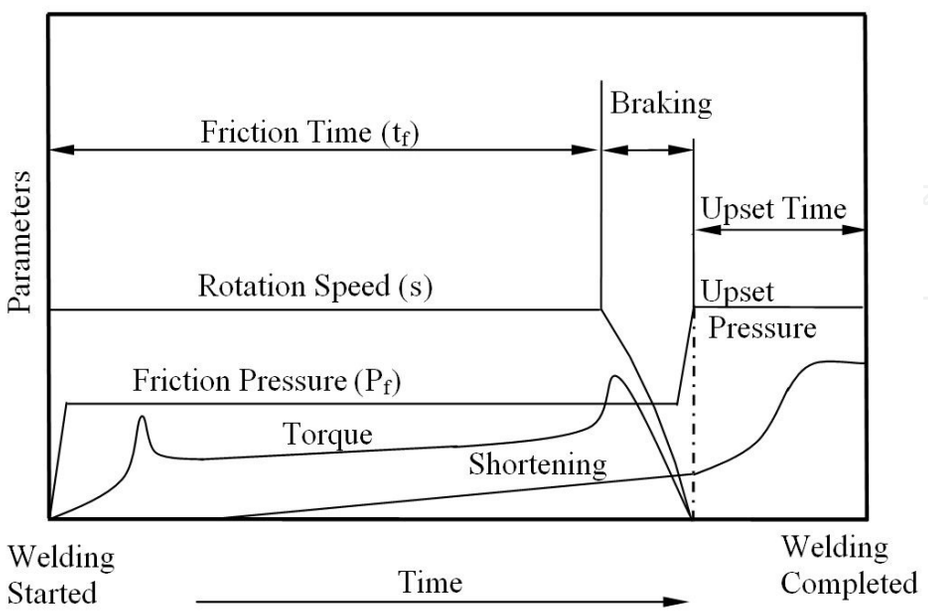

Figure 2. Parameters for Continuous Drive Friction Welding

http://dx.doi.org/10.5772/51130

In the inertia welding method, the second component is held stationary for welding, while one of the components is clamped in a spindle chuck, usually with attached fly wheels. The fly wheel and chuck assembly is rotated at a certain speed (s) to store a predetermined amount of energy. Then, the drive to the flywheel is declutched, and the two components are brought together under axial pressure (P_f) for welding. Friction between the parts decelerates the flywheel converting stored energy to frictional heat.

Vill, Kinley and Fomichev [2-4] studied the friction welding set-up and the strength of the joints. Murti et al. [5] directed a study about parameter optimisation in friction welding of dissimilar materials. Yılbas et al. [6] investigated the mechanical and metallurgical properties of friction welded steel-aluminium and aluminium-copper bars. Yılbas et al. [7] investigated the properties of friction-welded aluminium bars. Rhodes et al. [8] examined microstructure of 7075 aluminium using friction stir welding. Fukumoto et al. [9, 10] investigated amorphization process between aluminium alloy and stainless-steel by friction welding.

Then, Sahin and Akata [11] studied joining of plastically deformed steel (carburising steel) with friction welding. Sahin and Akata [12] carried out an experimental study on joining medium-carbon steel and austenitic-stainless steel with friction welding. Sahin [13, 14] studied joining austenitic-stainless steel with friction welding. Rhodes et al. [15] examined microstructure of 7075 aluminium using friction stir welding. Ouyang et al. [16] investigated microstructural evolution in friction stir welding of 6061 aluminium alloy (T6-temper condition) and copper. Maalekian M [17] performed a study on Friction Welding of dissimilar materials.

Surface cleanliness in terms of contaminants, especially grease, reduces the quality of joints. Furthermore, the cleanliness of the parts must be considered as important. Therefore, the ends of the parts were cleaned with acetone prior to the welding process to minimize the effect of organic contamination in the welding zone. However, the aim of this study is to investigate experimentally the microstructural and mechanical properties of friction welded aluminium-steel and aluminium-copper joints.

2. The experimental procedure

2.1. Material

In the experiments, AISI 304 austenitic-stainless steel and aluminium materials were used. The chemical composition and tensile strength of austenitic stainless steel is given in Tables 1. Chemical composition obtained by chemical analysis and tensile strength of aluminium and copper are given in Tables 2 and 3, respectively.

Material	% C	% P	% S	% Mn	% Si	% Cr	% Ni	Tensile Strength (MPa)
AISI 304 (X5CrNi1810)	0,07	0,045	0,030	2,0	1,0	17 - 19	8,5 – 10,5	825

Table 1. Chemical composition and tensile strength of austenitic-stainless steel [18].

Aluminium %Sn	%Pb	%Zn	%Mn	%Fe	%Ni	%Si	%Mg	%Sb	%Cr	%Ti	%Cu	%Al	Tensile Strength (MPa)
0,00500	0,03360	1,14000	0,11800	0,57400	0,01220	0,55400	0,17100	0,00300	0,02420	0,01340	0,59300	96,76000	200

Table 2. Chemical Compositions of Aluminium Used in the Experiments.

Copper	%Sn	%Pb	%Zn	%P	%Mn	%Fe	%Ni	%Si	%Mg	%Al	%Bi	%S	%Sb	%Cu	Tensile Strength (MPa)
	0,00222	<0,00200	<0,00100	0,00137	<0,00050	0,0381	<0,00100	0,00745	0,00376	0,00500	<0,00050	0,00251	<0,00200	99,93	300

Table 3. Chemical Compositions of Copper Used in the Experiments.

2.2. Geometry of Parts

Specimens were machined from materials according to geometry (Figure 3).

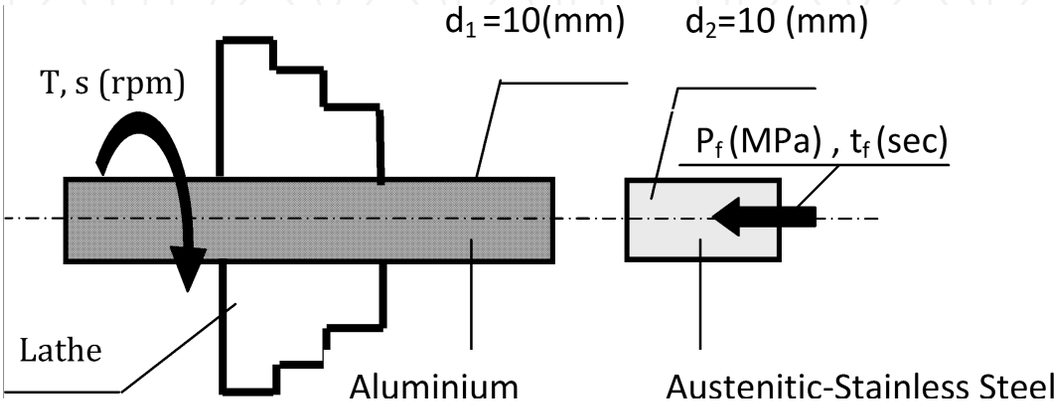

Figure 3. Equal Section Parts used in the experiments.

http://dx.doi.org/10.5772/51130

2.3. Experimental Set-up

An experimental set-up was designed and constructed as a continuous drive type. A solenoid valve and electrical control circuit was designed and constructed to control friction time and pressure in the set-up, thus allowing process control. The friction welding set-up is shown in Figure 4.

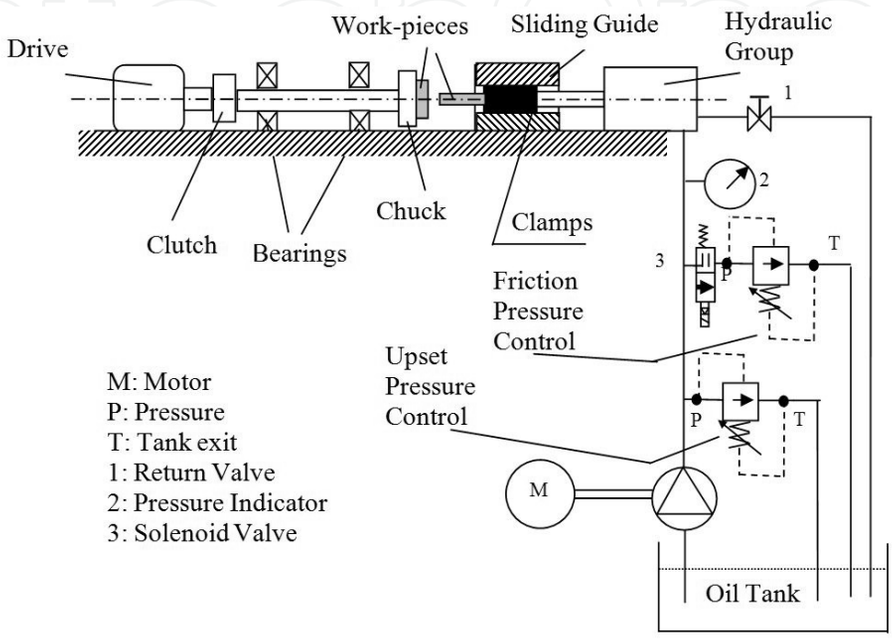

Figure 4. Continuous drive friction welding set-up.

The set-up was designed and constructed according to the principals of continuous drive welding machines. A drive motor with 4 kW power and 1410 rpm was selected as adequate for the torque capacity in friction welding of steel bars within 10 mm diameter taking into account the friction and the upset pressures. Friction and upset pressures can be seen on number2 pressure indicator, and the stages of the welding sequences are controlled by the number3 solenoid valve driven by an external timer.

Friction time, friction pressure and upset pressure have a direct effect on the tensile strength of joints. Therefore, linear statistical analysis was used in order to discover the effect of factors that have a significant role on the experimental results of previous studies [5, 6, 16].

3. Friction welded stainless steel and aluminium materials

Parameters having the least error by using the method of least squares were taken as the optimum welding parameters. Optimum parameters found in a previous different study [19] were used in the experiments (friction time= 4 sec., friction pressure= 30 MPa., upset time = 12 sec. and upset pressure = 60 MPa).

Subsequently, tensile tests, micro-hardness tests and metallurgical examinations were applied to the welded specimens.

3.1. Tensile Tests

Optimum parameters were found using statistical analysis for the welded parts. Later, many parts were machined and welded using the optimum parameters, and then these specimens were further tested. Effects of friction time and friction pressure on the strength of joints were examined in welding of equal diameter parts. Upset time was kept constant. The strength of joints was determined by tensile tests, and the results were compared with those of fully machined specimens. Tensile strength of the joints was estimated dividing the ultimate load by area of 10 mm diameter specimen. The relation obtained between tensile strength versus friction time and friction pressure is shown graphically in Figures 5 and 6.

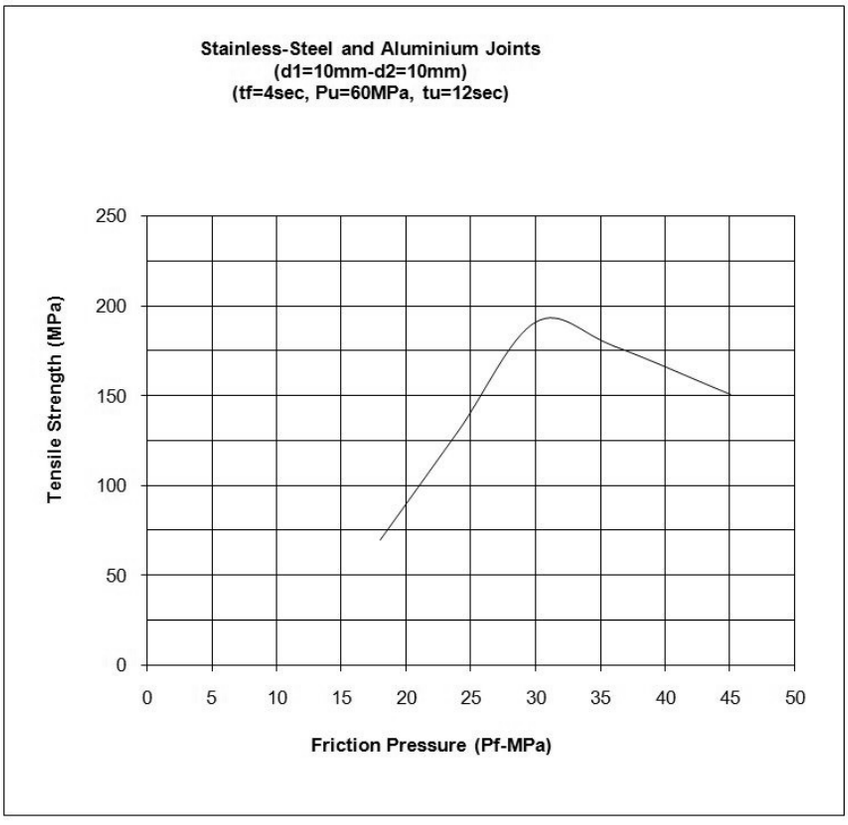

Figure 5. Relation between Tensile Strength versus Friction Pressure.

As friction time and friction pressure for the joints are increased, tensile strength of the joints increases (Figures 5 and 6). But, strength of the joints passes through a maximum, then, when friction time and friction pressure for the joints are increased, tensile strength of the joints decreases (Figures 5 and 6). Maximum strength obtained in the joints has about 94% that of aluminium parts having the weakest strength. Thus, it is shown that friction time and friction pressure have a direct effect on joint strength.

http://dx.doi.org/10.5772/51130

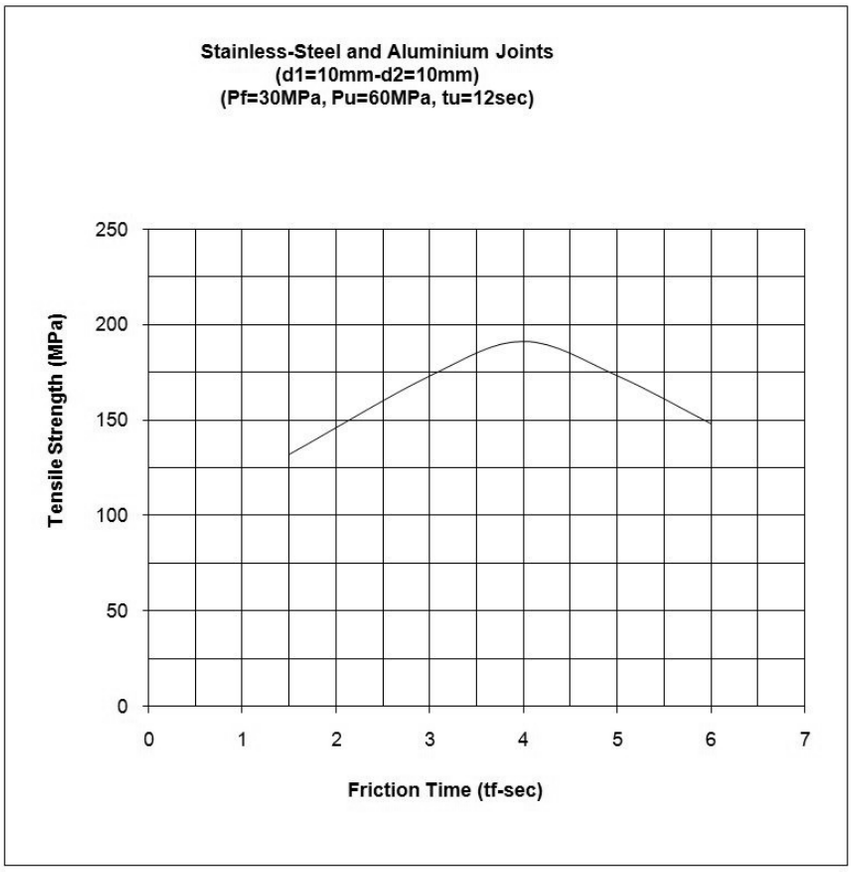

Figure 6. Relation between Tensile Strength versus Friction Time

3.2. Microstructure of Welded Parts

The photo and the macro-photo of the joint is shown in Figures 7 and 8,while the micro-structure-photos in the parent metals and interface region of the joints are shown in Figures 9, 10 and 11.

x 3

Figure 7. Photo of joint

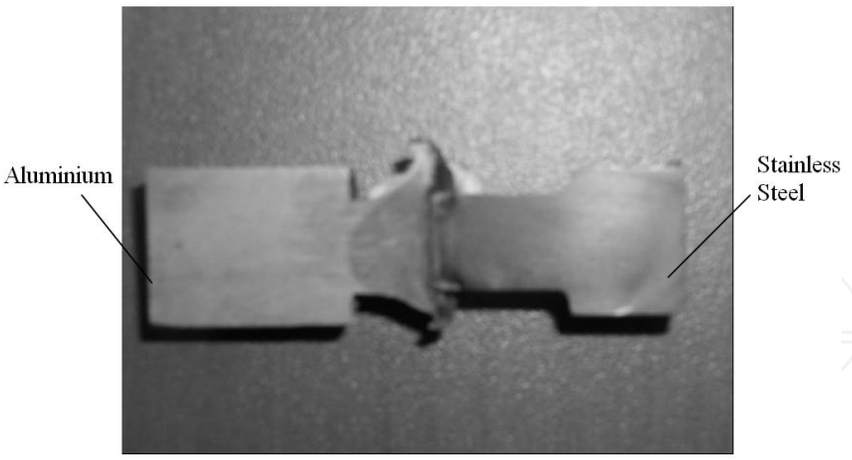

x 3

Figure 8. Macro-photo of joint

As shown in Figures 7 and 8, axial shortening in the aluminium side is much more than that of the stainless-steel side. However, the stainless steel was hardly ever deformed because the melting temperature of aluminium is lower than that of stainless-steel. Therefore, the weld flash consists of aluminium at the interface.

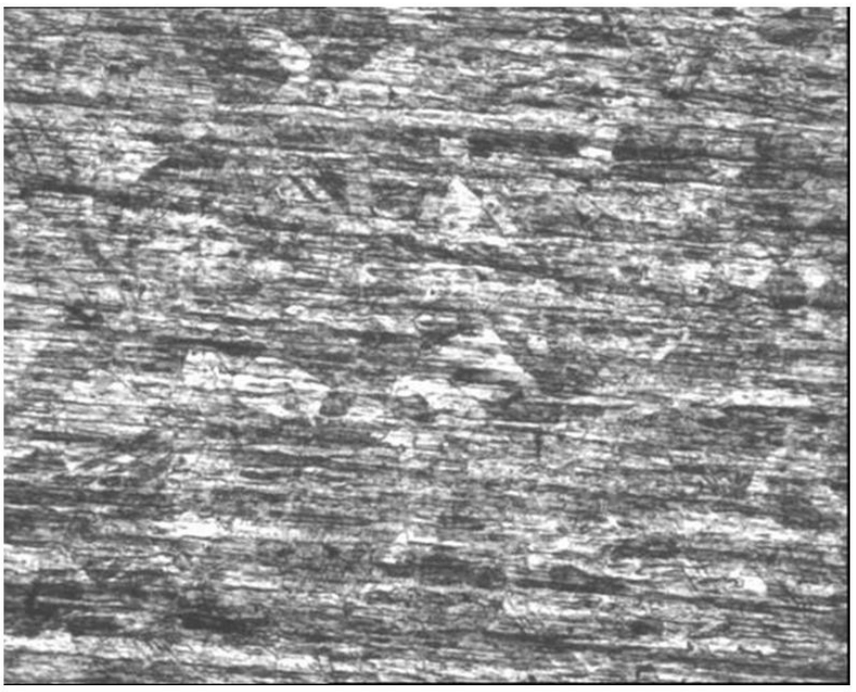

x 1000

Figure 9. Micro-photo of stainless-steel

http://dx.doi.org/10.5772/51130

The microstructure of the base metal consists of austenitic grain structure.

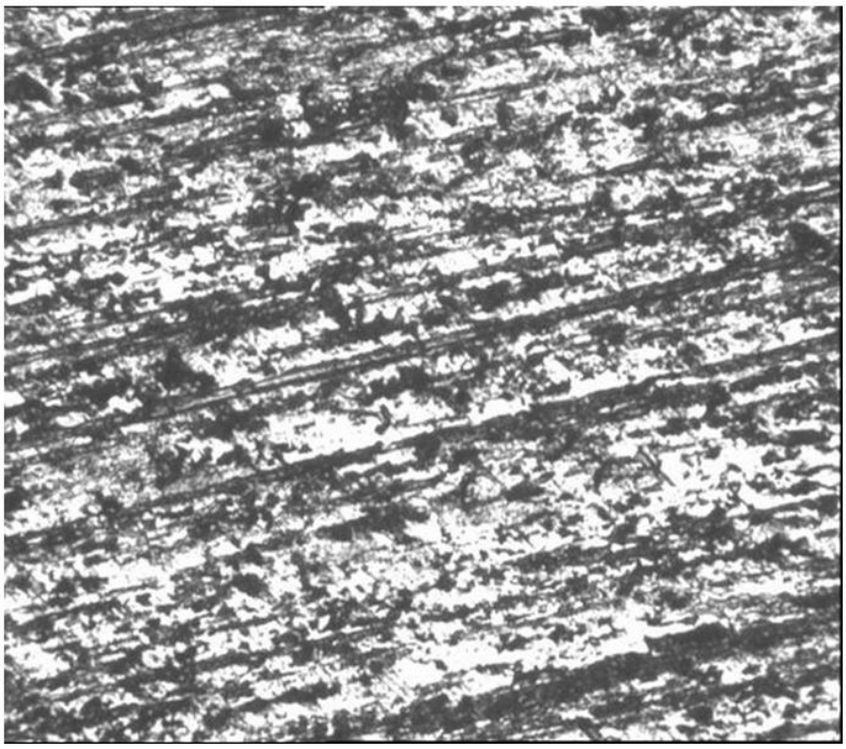

x 1000

Figure 10. Micro-photo of aluminium

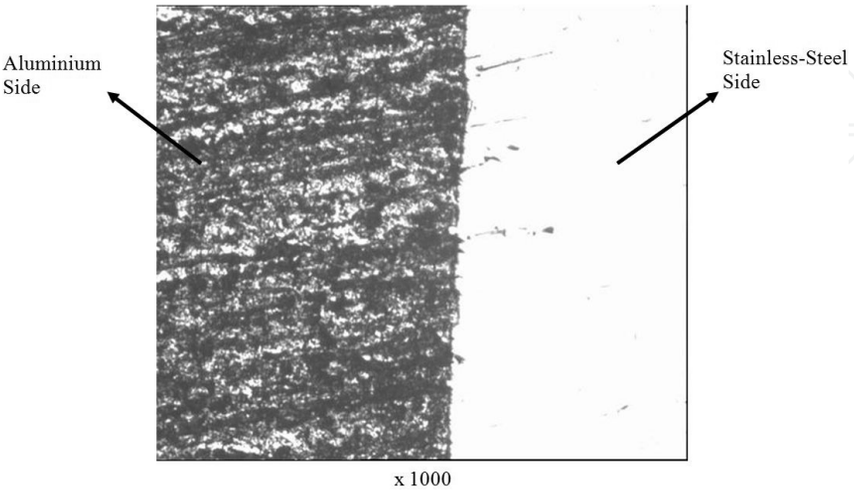

Figure 11. Micro-photo of interface region in joints

Micro-photographs (Figs. 9-11) show that aluminium was greatly deformed with grains elongated and refined near the weld interface. Stainless steel was slightly deformed and partly transformed at the faying surface from austenite to martensite owing to hard friction. Constituent elements of both materials had interdiffused through the weld interface, and intermetallic compounds such as FeAl and Fe_3Al, were formed at the weld interface.

3.3. EDX Analysis of Joints

Scanning electron microscopy (SEM) and energy dispersive X-ray (EDX) analysis were performed in order to investigate the phases that occur during welding at the welding interface. Observations were realized with a 25 kV field effect scanning electron microscope (SEM-JEOL JSM 5410 LV microscopy) associated to an EDS (energy dispersive X-ray spectroscopy) analysis. EDS point analysis was used in the examinations. The software allowed piloting of the beam, scanning along a surface or a line to obtain X-ray cartography or concentration profiles by elements, respectively. SEM microstructure of interface region in the friction welded steel-aluminium joint and EDX analysis results are given in Figure 12, while distribution of elements within the determined location are shown in Table 4. EDS analysis was carried out for various points of the SEM image.

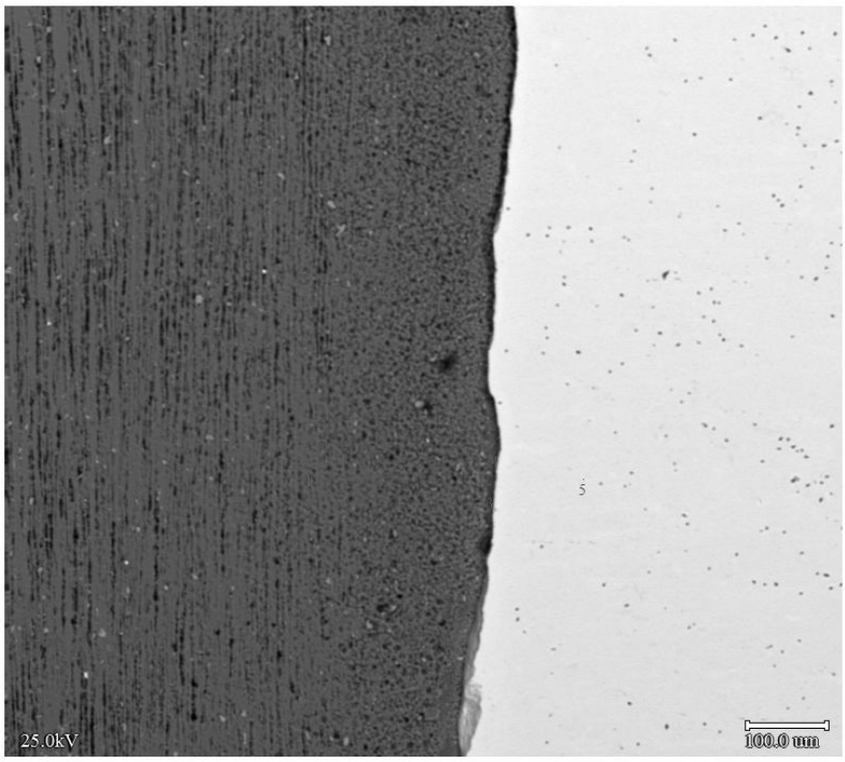

(a) SEM microstructure of joint interface.

http://dx.doi.org/10.5772/51130

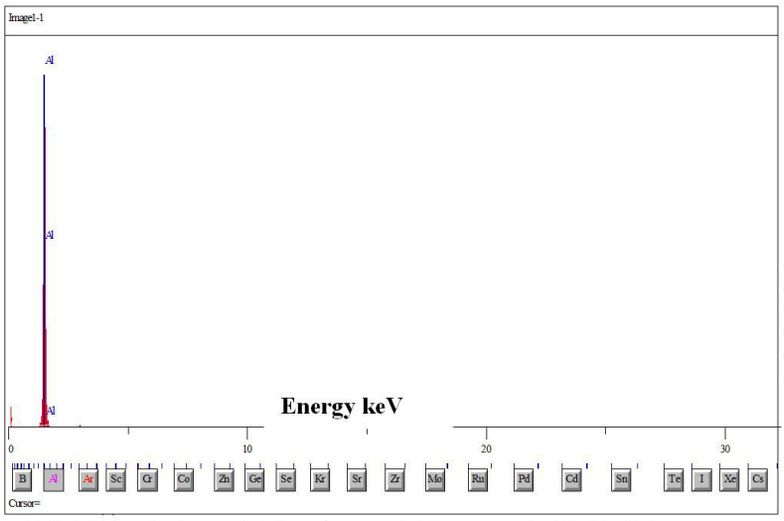

(b) EDX analysis result taken from point 1 represented to SEM image

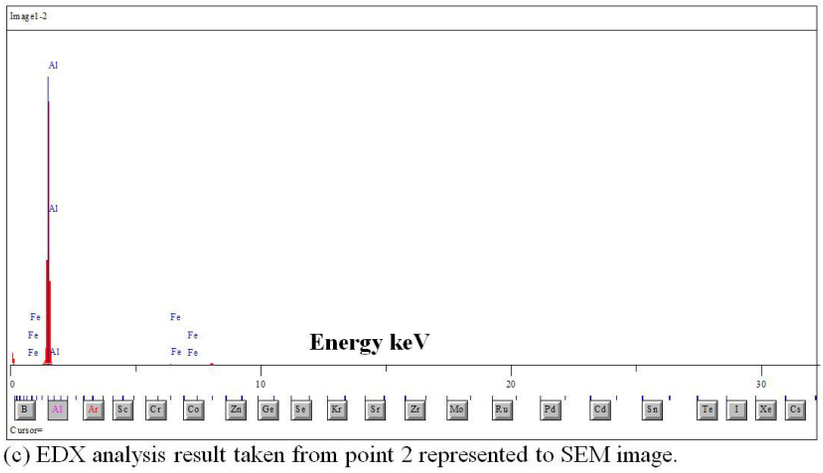

(c) EDX analysis result taken from point 2 represented to SEM image.

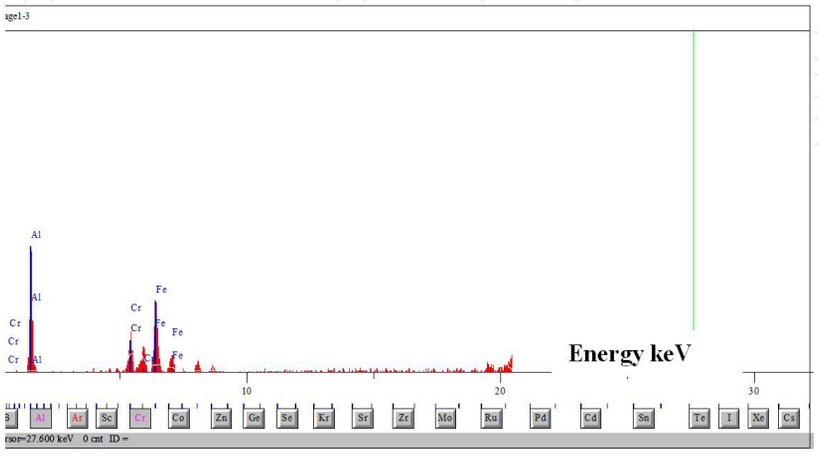

(d) EDX analysis result taken from point 3 represented to SEM image.

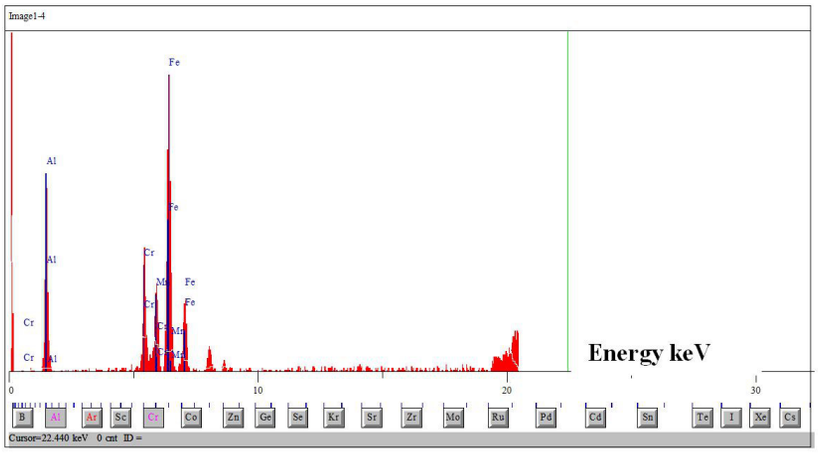

(e) EDX analysis result taken from point 4 represented to SEM image

Figure 12. SEM microstructure of interface region in the friction welded steel-aluminium joint and EDX analysis results.

Points	Elements	Line	Intensity (c/s)	Conclusion
1	Al	Ka	1928.84	100.000wt.%
				100.000wt.%Total
2	Al	Ka	1201.79	97.792wt.%
	Fe	Ka	10.30	2.208wt.%
				100.000wt.%Total
3	Al	Ka	57.68	36.742wt.%
	Cr	Ka	34.29	17.651wt.%
	Fe	Ka	60.68	45.607wt.%
				100.000wt.%Total
4	Al	Ka	97.01	21.117wt.%
	Cr	Ka	79.18	11.282wt.%
	Mn	Ka	76.10	12.472wt.%
	Fe	Ka	255.17	55.128wt.%
				100.000wt.%Total
5	Cr	Ka	370.48	18.189wt.%
	Fe	Ka	958.19	75.092wt.%
	Ni	Ka	58.40	6.719wt.%
				100.000wt.%Total

Table 4. EDS point analysis results according to SEM microstructure.

Fig. 12(a) shows EDX analysis points defined on the SEM microstructure in interface region of the friction welded St-Al joints. Fig. 12 (b), (c), (d) and (e) illustrate the EDX analysis results taken from the points 1,2,3 and 4 represented to St-Al joint, respectively. Then, Table 4

shows the EDS point analysis results represented to SEM. The EDS results confirm that St-Al joints contain some intermetallic compounds. Therefore, formation of brittle intermetallic compounds degrades the strength of the joints.

3.4. Hardness Variations of Welded Parts

Strength of the joints is related to hardness variation within the HAZ. Hardness variation was obtained under 500 g load by micro hardness (Vickers) testing, and measuring locations are shown in Figure 13. Hardness variations on horizontal and vertical distance from the centre in the welding zone of joints are shown in Figures 14 and 15.

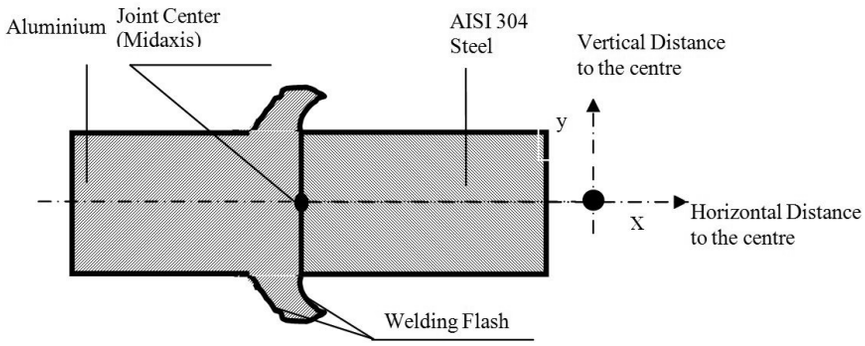

Figure 13. Hardness test orientation.

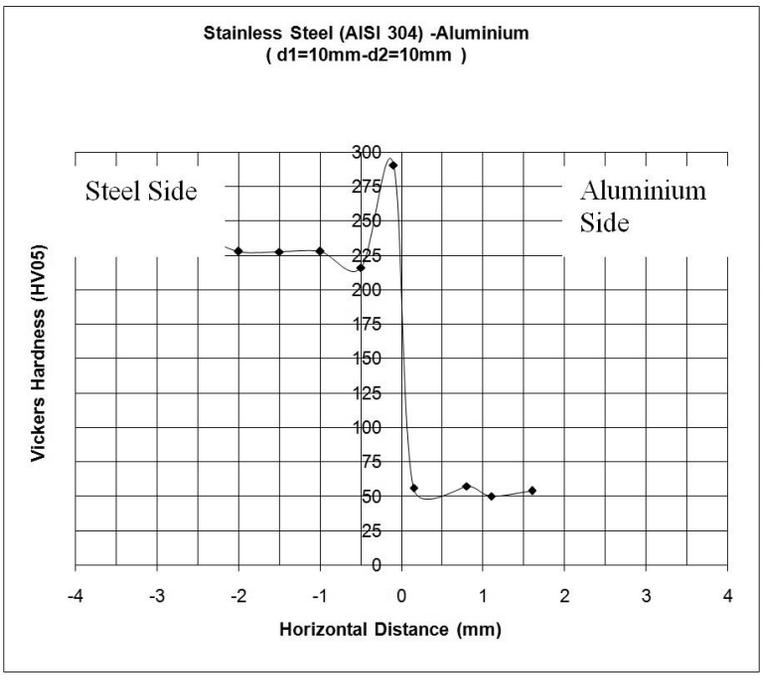

Figure 14. Hardness Distribution on the Horizontal Distance of Joints.

There are often significant differences between the tensile strength and hardness of the A heat affected zone (HAZ) the unaffected area of the welded component. The reduction in tensile strength of the HAZ under controlled conditions, particularly with the non-heat treatable alloys, can be somewhat predictable. The reduction in tensile strength of the HAZ for the heat treatable alloys is more susceptible to welding conditions and can be reduced below the required minimum requirement if excessive heating occurs during the welding operation.

Micro-hardness test results with respect to the horizontal distance from the center are shown in Fig.14. Increase in hardness corresponds to the steel side. HAZ with a small width was formed, resulting in softening of the aluminium alloy. As the aluminium used in the present study was a cold drawn bar, it was already work hardened before the friction welding procedure. The aluminium recovered and recrystallised as a result of friction heat and deformation, thus was slightly softened.

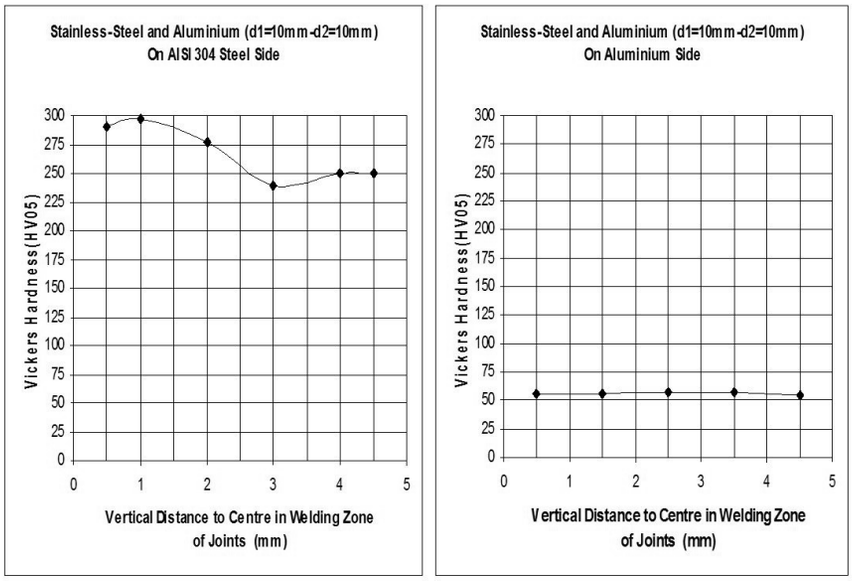

Figure 15. Hardness Distribution on the Vertical Distance of Joints.

As shown in Fig. 15(a), the hardness on the stainless-steel side of the joints decreases as it is advanced towards the end of the parts. On the other hand, hardness on the aluminium side of the joints did not change significantly (Fig. 15(b)).

4. Friction welded aluminium and copper materials

Parameters having the least error by using the method of least squares were taken as the optimum welding parameters. Optimum parameters found in a previous different study [20] were found as; (60 MPa) for friction pressure, (120 MPa) for upset pressure, (12 sec) for upset time and (2,5 sec) for friction time.

http://dx.doi.org/10.5772/51130

Subsequently, tensile tests, micro-hardness tests and metallurgical examinations were applied to the welded specimens.

4.1. Tensile Tests

Optimum parameters for welded parts.were found using statistical analysis. Then, parts machined were welded using these optimum parameters. Effects of friction time and friction pressure on strength of the joints were examined welding parts with equal diameter. Upset time was kept constant. The strength of joints was determined by tensile tests, and the results were compared with those of fully machined specimens. Three specimens were tested at each condition and average of three specimens is presented. Tensile strength of the joints was estimated dividing the ultimate load by the area of the 10 mm diameter specimen. The relation obtained between tensile strength versus friction time and friction pressure is shown graphically in Figures 16 and 17.

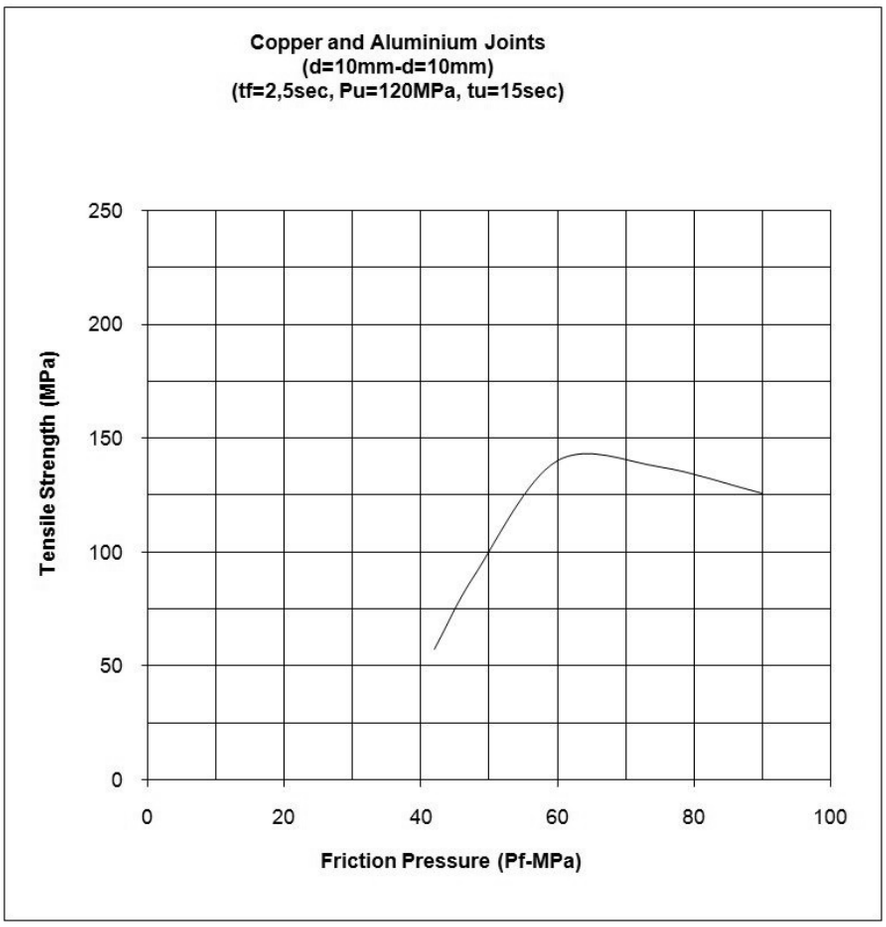

Figure 16. Relation between Tensile Strength versus Friction Pressure.

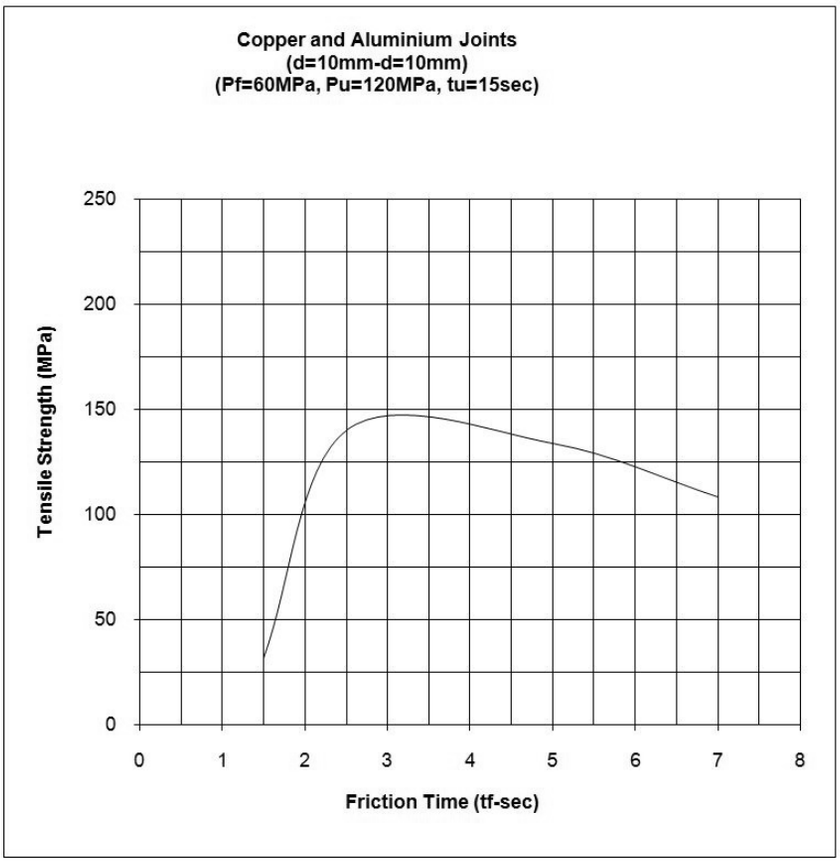

Figure 17. Relation between Tensile Strength versus Friction Time.

As the friction time and pressure for the joints is increased, tensile strength of the joints increases up to a peak strength then decreases with further increase in friction time and pressure (Figures 16 and 17). Peak strength corresponds to about 70% that of aluminium parts and 50% that of copper parts. A grey layer was observed at the fracture surfaces of welded parts. This layer results in a decrease in the strength of the joints.

4.2. Microstructure of Welded Parts

As regards joints, the photo and the macro-photo of the joint is shown in Figures 18 and 19. Then, the microstructure-photos in the parent metals and interface region of the joints are shown in Figures 20, 21, and 22.

It can be seen that the axial shortening on the aluminium side is more than that on copper side (Figures 18 and 19). Thus, the aluminium material has experienced weld flash at the interface. This is due to the fact that melting point of aluminium is lower than that of copper.

http://dx.doi.org/10.5772/51130

Figure 18. Macro-photo of Joint.

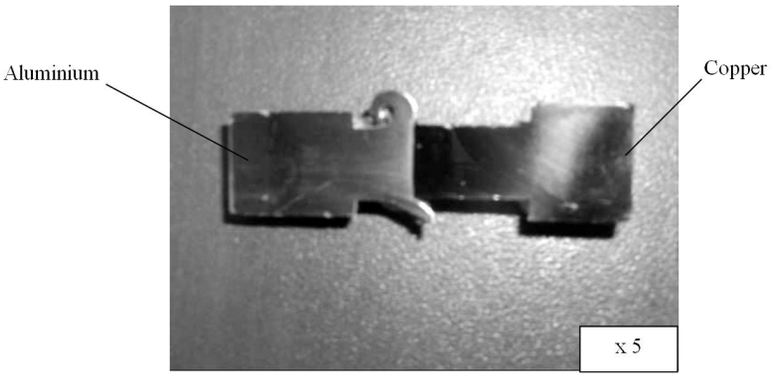

Figure 19. Macro-photo of Joint.

Figure 20. Micro-photo of Copper.

Figure 21. Micro-photo of Aluminium.

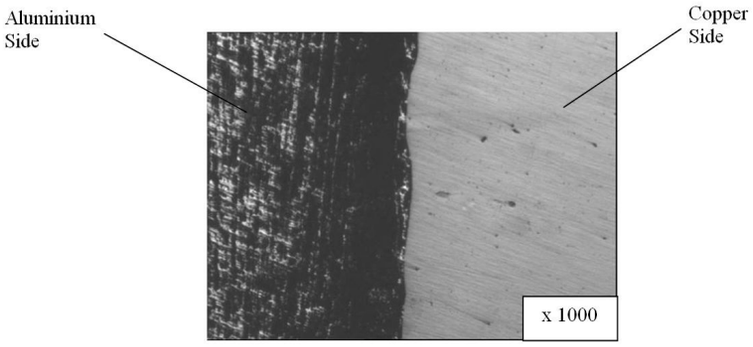

Figure 22. Micro-photo of Interface Region in Joints.

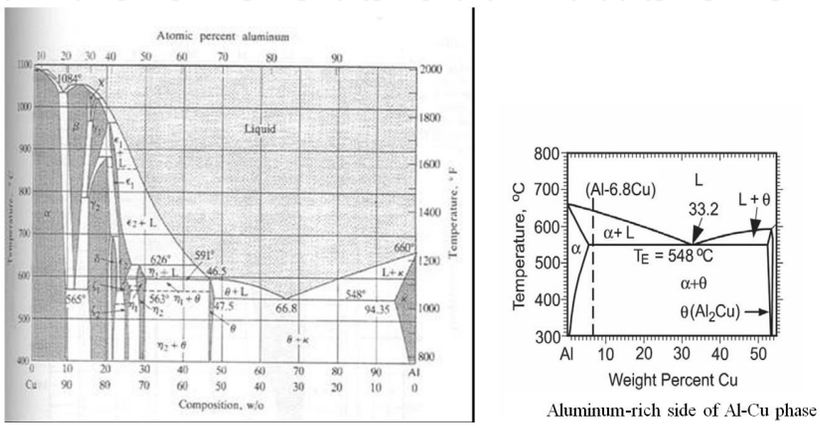

Figure 23. Al–Cu Binary Equilibrium Phase Diagram [17].

http://dx.doi.org/10.5772/51130

The copper substrate exhibits an irregular grain (Fig. 20). The grains of aluminium are elongated along the rolling direction (Fig. 21). The microphotograph of aluminium also contains insoluble particles of $FeAl_3$ (black). Relatively coarse $CuAl_2$ grains are clearly observed at the transition zone of the copper side [21, 22, 23 and 24].

Microstructural observations showed that a mixed layer of aluminium and copper that includes brittle intermetallic compounds such as $CuAl_2$, CuAl, and Cu_9Al_4 are formed in a dissimilar aluminium alloy/copper weld. The formation of intermetallic compounds can be understood by an analysis of the Al–Cu binary phase diagram (Fig. 11) [24].

4.3. EDX Analysis of Joints

Scanning electron microscopy (SEM) and energy dispersive X-ray (EDX) analysis were performed in order to investigate the phases that occur at the welding interface. Observations were realized with a 25 kV field effect scanning electron microscope (SEM- JEOL JSM 5410 LV microscopy) coupled to EDS (energy dispersive X-ray spectroscopy) analysis. EDS point analysis was used in the examinations. The software allowed piloting the beam to scan along a surface or a line so as to obtain X-ray cartography or concentration profiles by elements. SEM microstructure of the interface region in the friction welded copper-aluminium joint and EDX analysis results are given in Figure 24, while distribution of elements within the determined location are shown in Table 5. EDS analysis was carried out for various points of the SEM image.

Points	Elements	Line	Intensity (c/s)	Conclusion
1	Al	Ka	1054.36	89.113wt.%
	Fe	Ka	36.54	6.523 wt.%
	Cu	Ka	15.65	4.364 wt.%
				100.000wt.%Total
2	Al	Ka	1013.86	100.000wt.%
				100.000wt.%Total
3	Al	Ka	891.13	80.581wt.%
	V	Ka	0.96	0.115wt.%
	Fe	Ka	23.84	3.537wt.%
	Cu	Ka	65.64	15.767wt.%
				100.000wt.%Total
4	Cu	Ka	883.70	100.000wt.%
				100.000wt.%Total
5	Cu	Ka	790.24	100.000wt.%
				100.000wt.%Total

Table 5. EDS Point Analysis Results according to SEM Microstructure.

Fig. 24 shows EDS analysis points defined on the SEM microstructure in interface region. Table 5 illustrates the EDS analysis results taken from the points 1, 2, 3, 4 and 5, respectively represented by SEM.

The EDS results confirm that Cu-Al joints contain some intermetallic compounds. Formation of these brittle intermetallic compounds degrades the strength of the joints.

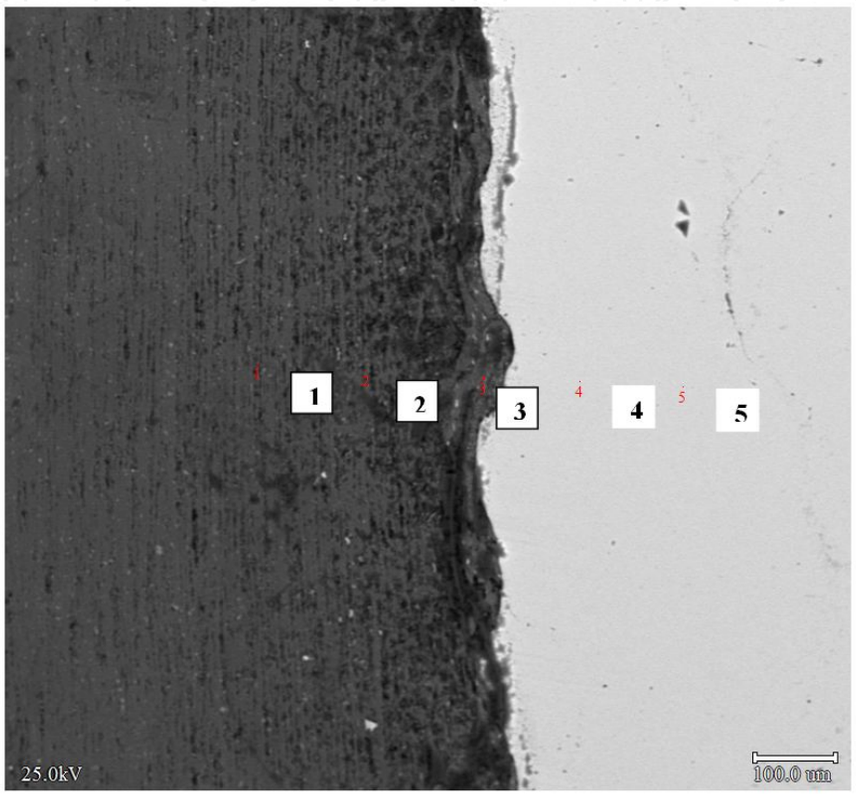

Figure 24. SEM Microstructure of Interface Region in the Friction Welded Copper-Aluminium Joint and EDX Analysis Markers

4.4. Hardness Variations of Welded Parts

Strength of the joints is related to hardness variation within the HAZ. Hardness variation was obtained under 200 g loads by micro hardness (Vickers) testing. Micro-hardness test results with respect to the horizontal distance from the centre are shown in Fig. 25.

As the aluminium used in the present study was a cold drawn bar, it was already work hardened before friction welding. Aluminium recovered and recrystallised as a result of frictional heat and deformation, thus was slightly softened. Hardness variations on the copper side are more than those on the aluminium side. This variation is due to comparatively high thermal conductivity of copper.

http://dx.doi.org/10.5772/51130

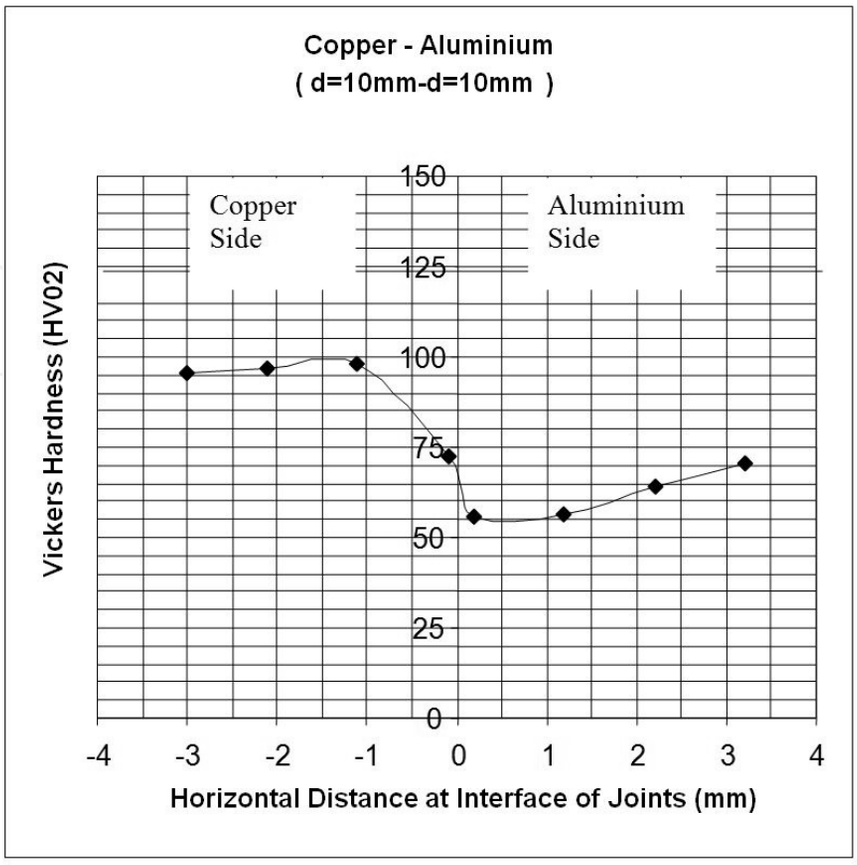

Figure 25. Hardness Results on Horizontal Distance at Interface of Joints

5. Conclusions

In the present study, austenitic-stainless steel (AISI 304)-aluminium and aluminium-copper materials were welded successfully. The welding process was investigated by tensile testing, microstructural observation, EDS measurements and hardness testing. As a result:

- Optimum welding parameters should be properly selected in the friction welding of parts.

- Tensile strengths for austenitic-stainless steel and aluminium parts yielded a positive result when compared to those of the base metals. The joint strength increased and then decreased after reaching a maximum value, with increasing friction time. Sufficient heat to obtain a strong joint could not be generated with a shorter friction time. A longer friction time caused the excess formation of an intermetallic layer. However, some of the welds showed poor strength depending on some accumulation of alloying elements at the interface, which are the result of a temperature rise and the existence of intermetallic layers such as FeAl.

- Although tensile strength for copper and aluminium joints were generally acceptable when compared with those of the base metals, some of the welds showed poor strength as a result of the accumulation of alloying elements at the interface. This was the result of temperature

rise and the existence of a grey layer. This grey layer formed due to heat dissipation in friction welding and was found to contain a considerable amount of intermatallic compounds.

- The presence of contaminants at the interface of the metals reduces the joint quality. No significant effect was observed on welding properties with respect to the surface finish operations.

- In the microphotos, the broken up aluminium oxide film resulted in increased deformation at the interface. Formation of an oxide in the joints causes a barrier that prevents diffusion.

- The difference in weight of alloying elements can be clearly seen by analyzing spectrum of elements. EDX measurements clearly show that St-Al and Cu-Al joints consist of some intermetallic compounds. The intermetallic layer formed constituted mainly of FeAl, Fe_3Al, $CuAl_2$, CuAl, and Cu_9Al_4 together with some Al and Cu (saturated solid solution of Al in copper). Copper particles embedded in aluminium were observed. Then, it can be imparted in terms of galvanic effect that Fe_3Al particles are anodic to the matrix in St-Al joints. However, the copper band on either side of the grain boundary is dissolved while the grain boundary is cathodic due to the $CuAl_2$ and Cu_9Al_4 precipitates.

- Hardness of steel and aluminium materials in the vicinity of the weld interface was higher than that of the base metals. Then, in Al-Cu joints, hardness variations on the aluminium side were lower than those on the copper side as expected.

- Aluminium alloys are highly reflective and decorative. The high reflectivity is an inherent feature of aluminium; pure bulk aluminium can go up to 92 % total reflection. Alloying reduces this value slightly.

- The main value of this paper is to contribute and fulfil the detailed the Welded Aluminium Alloys that are being studied so far in the literature.

Acknowledgements

The author wishes to thank Hema Industry / Çerkezköy, the Mech. Eng. Dept. of Trakya University, Edirne and Metall. and Mater. Eng. Dept. of Yildiz University, Istanbul-Turkey for their help in the experimental and microstructure studies.

Author details

Mumin Sahin* and Cenk Misirli

*Address all correspondence to: mumins@trakya.edu.tr

Dept. of Mechanical Eng., Trakya University, Turkey

http://dx.doi.org/10.5772/51130

References

[1] Polmear, . J. (1995). *Light Alloys*, Arnold.

[2] Vill, V. I. (1962). Friction Welding of Metals. AWS, New York.

[3] Kinley, W. (1979, Oct). Inertia Welding: Simple in Principle and Application. *Welding and Metal Fabrication*, 585-589.

[4] Fomichev, N. I. (1980). The Friction Welding of New High Speed Tool Steels to Structural Steels. *Welding Production*, 35-38.

[5] Murti, K. G. K., & Sundaresan, S. (1983, June). Parameter Optimisation in Friction Welding Dissimilar Materials. *Metal Construction*, 331-335.

[6] Yılbaş, B. S., Şahin, A. Z., Kahraman, N., & Al-Garni, A. Z. (1995, Feb 15). Friction Welding of St- Al and Al- Cu Materials. *Journal of Materials Processing Tecnology*, 49(3-4), 431-443.

[7] Yılbaş, B. S., Şahin, A. Z., Çoban, A., & Abdul, Aleem. B. J. (1995). Investigation into the Properties of Friction-Welded Aluminium Bars. *Journal of Materials Processing Technology*, 54, 76-81.

[8] Rhodes, C. G., Mahoney, M. W., Bingel, W. H., Spurling, R. A., & Bampton, C. C. (1997). Effects of Friction Stir Welding on Microstructure of 7075 Aluminium. *Scripta Materialia*, 36(1), 69-75.

[9] Fukumoto, S., Tsubakino, H., Okita, K., Aritoshi, M., & Tomita, T. (2000). Amorphization by Friction Welding between 5052 Aluminum Alloy and 304 Stainless Steel. *Scripta Materialia*, 42, 807-812.

[10] Fukumoto, S., Tsubakino, H., Okita, K., Aritoshi, M., & Tomita, T. (1999, September). Friction Welding Process of 5052 Aluminium Alloy to 304 Stainless Steel. *Materials Science and Technology*, 15, 1080-1086.

[11] Sahin, M., & Akata, H. E. (2003). Joining with Friction Welding of Plastically Deformed Steel. *Journal of Materials Processing Technology*, 142(1), 239-246.

[12] Sahin, M., & Akata, H. E. (2004). An Experimental Study on Friction Welding of Medium Carbon and Austenitic Stainless Steel Components. *Industial Lubrication & Tribology*, 56(2), 122-129.

[13] Sahin, M. (2005). An Investigation into Joining of Austenitic-Stainless Steels (AISI 304) with Friction Welding. *Assembly Automation*, 25(2), 140-145.

[14] Sahin, M. (2006). Evaluation of The Joint-Interface Properties of Austenitic-Stainless Steels (AISI 304) Joined by Friction Welding. Materials & Design, In Press, Corrected Proof, Available Online 28 July

[15] Rhodes, C. G., Mahoney, M. W., Bingel, W. H., Spurling, R. A., & Bampton, C. C. (1997). Effects of Friction Stir Welding on Microstructure of 7075 Aluminium. *Scripta Materialia*, 36(1), 69-75.

[16] Ouyang, J., Yarrapareddy, E., & Kovacevic, R. (2006). Microstructural Evolution In The Friction Stir Welded 6061 Aluminium Alloy (T6-Temper Condition) To Copper. *Journal of Materials Processing Technology*, 172, 110-122.

[17] Maalekian, M. (2007). Friction Welding- Critical Assessment of Literature. *Science and Technology of Welding & Joining*, 12(8), 738-759.

[18] Stahlschlüssel, (1995). Verlag Stahlschlüssel Wegst Gmbh

[19] Sahin, M. (2009). Joining of stainless-steel and aluminium materials by friction welding. *Int J Adv Manuf Technol*, 41, 487-497.

[20] Sahin, M. (2010). Joining of aluminium and copper materials with friction welding. *The International Journal of Advanced Manufacturing Technology*, 49(5-8), 527-534.

[21] Koberna, M., & Fiala, J. (1993). Intermetallic Phases Influencing The Behaviour of Al-Cu Joints. *Journal of Physics and Chemistry of Solids*, 54(5), 595-601.

[22] Braunovic, M., & Alexandrov, N. (1994). Intermetallic Compounds at Aluminium-to-Copper Electrical Interfaces: Effect of Temperature and Electric Current. *IEEE Transactions on Components, Packaging, and Manufacturing Technology-Part A,*, 17(1), 78-85.

[23] Lee, W. B., Bang, K. S., & Jung, S. B. (2005). Effects of Intermetallic Compound on The Electrical and Mechanical Properties of Friction Welded Cu/Al Bimetallic Joints during Annealing. *Journal of Alloys and Compounds*, 390(1-2), 212-219.

[24] ASM Handbooks, (2002). Alloy Phase Diagrams, ASM International, Materials Park, Ohio, 3